Motion generation by *Drosophila* mechanosensory neurons

M. C. Göpfert* and D. Robert

School of Biological Sciences, University of Bristol, Woodland Road, Bristol BS8 1UG, United Kingdom

Edited by A. James Hudspeth, The Rockefeller University, New York, NY, and approved February 5, 2003 (received for review December 12, 2002)

In *Drosophila melanogaster*, hearing is supported by mechanosensory neurons transducing sound-induced vibrations of the antenna. It is shown here that these neurons additionally generate motions that mechanically drive the antenna and tune it to relevant sounds. Motion generation in the *Drosophila* auditory system is betrayed by the auditory mechanics; the antenna of the fly nonlinearly alters its tuning as stimulus intensity declines and oscillates spontaneously in the absence of sound. The susceptibility of auditory motion generation to mechanosensory mutations shows that motion is generated by mechanosensory neurons. Motion generation depends on molecular components of the mechanosensory transduction machinery (NompA, NompC, Btv, and TilB), apparently involving mechanical activity of ciliated dendrites and microtubule-dependent motors. Hence, in analogy to vertebrate hair cells, the mechanosensory neurons of the fly serve dual, transducing, and actuating roles, documenting a striking functional parallel between the vertebrate cochlea and the ears of *Drosophila*.

Hearing is a particularly sensitive form of mechanosensation that relies on dedicated mechanosensory cells transducing sound-induced motions of nanometer and subnanometer range dimensions (reviewed in refs. 1–4). Hair cells, the nonneural, epithelial mechanoreceptors in vertebrate ears, achieve this sensitivity actively. These cells respond to mechanical stimuli by cell body contractions [mammalian outer hair cells (2, 4–6)] or active hair bundle twitches [lower tetrapod hair cells (3, 7, 8)], which, in turn, assist the minute motions induced by sound. The result is a positive mechanical feedback. Through their motility, hair cells actively augment those mechanical stimuli they have to transduce (2–8). This feedback impacts on cochlear mechanics. It nonlinearly alters mechanical tuning as the stimulus intensity declines, thereby improving the detection of faint, relevant sound (reviewed in refs. 2–8). In a quiet environment, in turn, excess feedback can lead to spontaneous oscillations, explaining the fascinating ability of the cochlea to spontaneously emit sound (9, 10). Nonlinearity and spontaneous oscillations have recently been documented for the auditory system of mosquitoes (11), putting forward the question of whether the auditory mechanosensory neurons that mediate hearing in insects mechanically assist audition in a hair cell-like way (12–15). Here, we dissect the auditory mechanics in *Drosophila melanogaster* and show that its mechanosensory neurons are motile.

In *Drosophila*, antennal hearing organs mediate the detection of conspecific songs (reviewed in refs. 16–18). The auditory sense organ, Johnston's organ, is located in the second segment of the antenna (Fig. 1*A*). The organ houses several hundred stretch-sensitive chordotonal sensilla, each comprising two to three primary neurons with ciliated dendrites (15, 19, 20). Stretching across an antennal joint, the sensilla connect the neurons to the third segment of the antenna (19, 20). This segment, together with its feather-like arista, constitutes the sound receiver (refs. 19 and 21; Fig. 1*A*). Being flexibly suspended by the antennal joint and the associated Johnston's organ, this external receiver acts like a simple spring-mass system and vibrates in response to the particle velocity component of sound (19, 21). When stimulated acoustically, the receiver moves as a rigid body; being stiffly coupled at its base and translating like a stiff rod, the arista twists the third segment of the antenna about the antennal joint (19, 21). Because of the direct proximity of the joint to Johnston's organ, the rotary vibrations of the receiver will alternately stretch and compress the chordotonal sensilla along their longitudinal axis, thereby directly activating the mechanosensory neurons (19–21).

Taking advantage of the accessible natural handle provided by the fly's external receiver on the one hand, and of the amenability of Johnston's organ to genetic manipulations (12, 20, 22, 23) on the other, we have investigated the *in situ* mechanical properties of mechanosensory neurons in a noninvasive way. Using laser Doppler vibrometry, we first evaluated the presence of nonlinearity and spontaneous oscillation activity, two key signatures of auditory motion generation, by analyzing the receiver's mechanics in WT flies. Then, we traced the underlying motor mechanism by using mechanosensory mutants (24, 25).

Materials and Methods

Flies. All WT measurements were made from the Oregon-R strain. The $nompA^2$, $nompC^2$, and btv^{5P1} mutations were examined in the homozygous condition, and the X-linked $tilB^2$ was tested in males. The respective genetic backgrounds *cn bw* (for $nompA^2$ and $nompC^2$), *w;* FRT^{40A} FRT^{G13} (for btv^{5P1}), and *y w* (for $tilB^2$) (24, 25) were used as controls.

Mechanical Measurements. Measurements were performed on a TMC (Peabody, MA) 78-443-12 vibration isolation table at room temperature (22–24°C). The flies were mounted ventrum-down on top of a holder with their wings and legs removed and their heads and halteres waxed to the thorax (19). The vibration velocity of the antennal receiver was measured in nonloading conditions by using a Polytec (Waldbronn, Germany) PSV-200 scanning laser Doppler vibrometer with an OFV-055 scanning head and an OFV-3001-S beam controller. All measurements were taken from the distal region of the arista (Fig. 1*A*), the vibrations of which reflect those of the entire receiver with respect to their frequency characteristics (19, 21). Control measurements on the second segment of the antenna (data not shown) established that all of the mechanical effects described in this study did not extend to the base of the antenna, ruling out the involvement of muscular activity. The laser signal was conditioned with antialiasing filters and digitized at a rate of 12.5 kHz by using an Analogic 16 Fast A/D board. To produce frequency spectra, groups of 3–5 (responses to sound) or 100 windows (spontaneous oscillations), each 650 ms in length, were collected, subjected to the Fast Fourier transform with a rectangular window, and subsequently averaged. Resonance frequency f_R was determined using least square fits on the function of a simple harmonic oscillator. The function was fitted either to the complex data, taking both magnitude and phase into account (responses to sound), or to the magnitude alone (spontaneous

This paper was submitted directly (Track II) to the PNAS office.

*To whom correspondence should be addressed. E-mail: m.gopfert@bristol.ac.uk.

www.pnas.org/cgi/doi/10.1073/pnas.0737564100

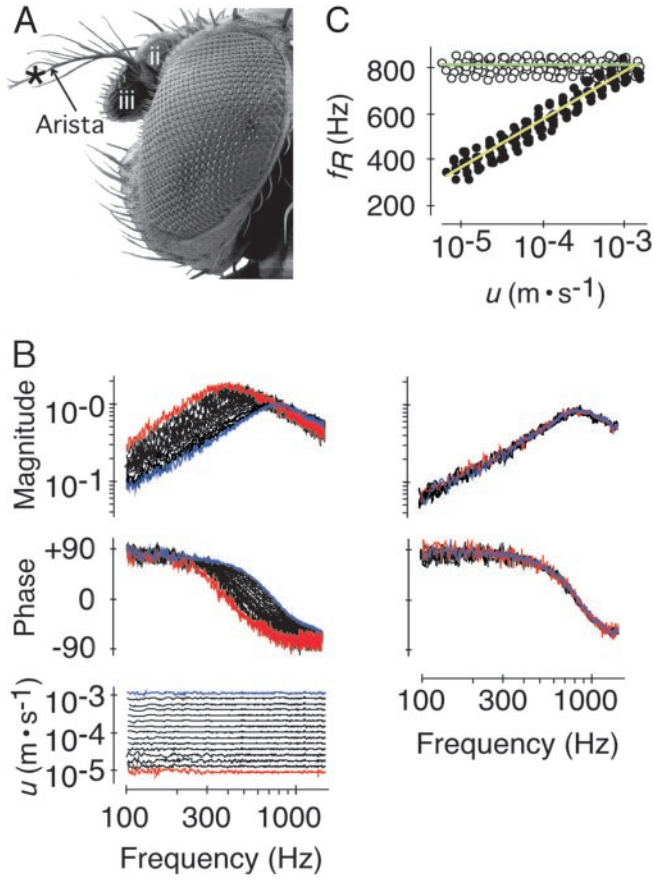

Fig. 1. Nonlinear response of the receiver in WT flies. (*A*) Lateral view of the head depicting the second and third antennal segments (ii and iii), the arista, and the measurement site (*). (*B*) Superimposed magnitude (*Top*) and phase responses (*Middle*) of a receiver stimulated at different stimulus particle velocities *u* (*Bottom*; see also for color convention) *in vivo* (*Left*) and *post mortem* (*Right*). Response magnitudes are given as ratio between the vibration velocity *v* and the stimulus particle velocity *u* ($m \cdot s^{-1}/m \cdot s^{-1}$); response phases are given in degrees (°). (*C*) f_R as a function of *u* as measured *in vivo* (●, yellow line) and *post mortem* (○, green line) ($n = 10$ flies). Lines, averaged logarithmic fits; slopes, *in vivo*: $+10.6 \pm 0.7$ Hz/dB ($r^2 = 0.99 \pm 0.00$, $P < 0.001$), *post mortem*: 0.0 ± 0.1 Hz/dB ($r^2 = 0.07 \pm 0.10$, $P > 0.05$).

oscillations). Velocities were given as amplitudes and averages were expressed as means ± SD.

Acoustic Stimulation. Sound-induced mechanical responses were obtained by exposing the animals to periodic chirp sounds (100- to 1,500-Hz bandwidth, 650-ms duration, flat particle velocity spectrum within ±1.5 dB). Stimulus signals were generated by using a computer-controlled Hewlett–Packard HP 33120A function generator, passed through a step-attenuator, amplified, and subsequently fed to a loudspeaker positioned 5 cm behind the animal. The particle velocity *u* of the acoustic stimulus was monitored at the position of the antenna by using an Emkay (Itasca, IL) NR 3158 miniature pressure-gradient microphone (for sound field descriptions, see ref. 19). Cross-calibration against a Brüel & Kjaer Instruments (Naerum, Denmark) 4138 pressure microphone under acoustic far field conditions (19) established the response of the pressure-gradient microphone to be flat within ±0.8 dB at frequencies between 100 and 1,500 Hz. By using the Polytec HLV software package, the input signal fed to the loudspeaker was adjusted until the particle velocity spectrum at the position of the antenna was flat within ±1.5 dB (Fig. 1*B Bottom*). To assess nonlinear effects in the mechanics of the receiver, the amplitude of the stimulus particle velocity *u* was arbitrarily varied in 3-dB steps within a range of 45 dB centered at a particle velocity of $\approx 10^{-4}$ $m \cdot s^{-1}$. Within this range of intensities, the transfer function between the microphone output and the loudspeaker input was independent from intensity, establishing linear characteristics for the experimental equipment used. Both laser and microphone signals were processed in the same way, and mechanical responses were calculated as transfer functions between the two signals.

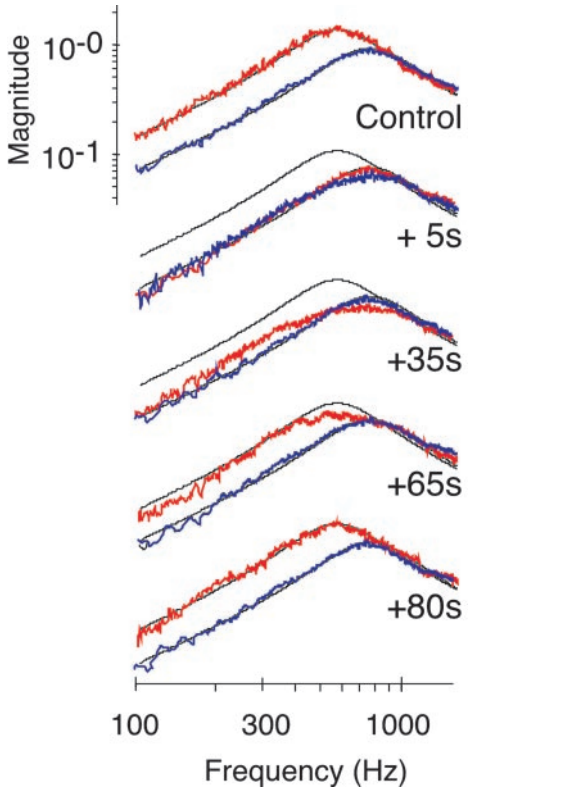

Fig. 2. Transient linearization of the response of the receiver after 20-s exposure to CO_2. Magnitude responses at two particle velocities [$u = 5 \times 10^{-4}$ m/s (red) and 1×10^{-3} m/s (blue)] before (control) and after exposure. Black lines, simple harmonic oscillator function fitted to the control responses. Response magnitude is as in Fig. 1*B*.

Results

Auditory Nonlinearity. Nonlinear effects in the auditory mechanics were assessed by analyzing intensity-dependent changes of the mechanical response of the receiver to sound. In WT flies, the mechanics of the antennal receiver was notably nonlinear; the resonant response of the receiver markedly moved in frequency when the stimulus intensity was altered (Fig. 1*B*). When the amplitude of the stimulus particle velocity was decreased stepwise from 10^{-3} m/s to 10^{-5} m/s, the resonance frequency (f_R) of the receiver gradually shifted down from 815 ± 37 Hz to 395 ± 46 Hz with an average slope of 10.6 Hz/dB ($n = 10$; Fig. 1 *B* and *C*). Such intensity-dependent shift of f_R is indicative of a stiffness nonlinearity; some components in the auditory system of the fly become more compliant as intensity declines. This nonlinear effect was found to depend on the physiological condition of the animal. First, the mechanics of the receiver became linear when measured postmortem. Responses to different stimulus intensities superimposed, with f_Rs clustering around 809 ± 34 Hz (Fig. 1 *B* and *C*). Second, linearization at frequencies ≈800 Hz also took place when the animals were transiently anesthetized by CO_2 (Fig. 2). The effect was revers-

NEUROSCIENCE

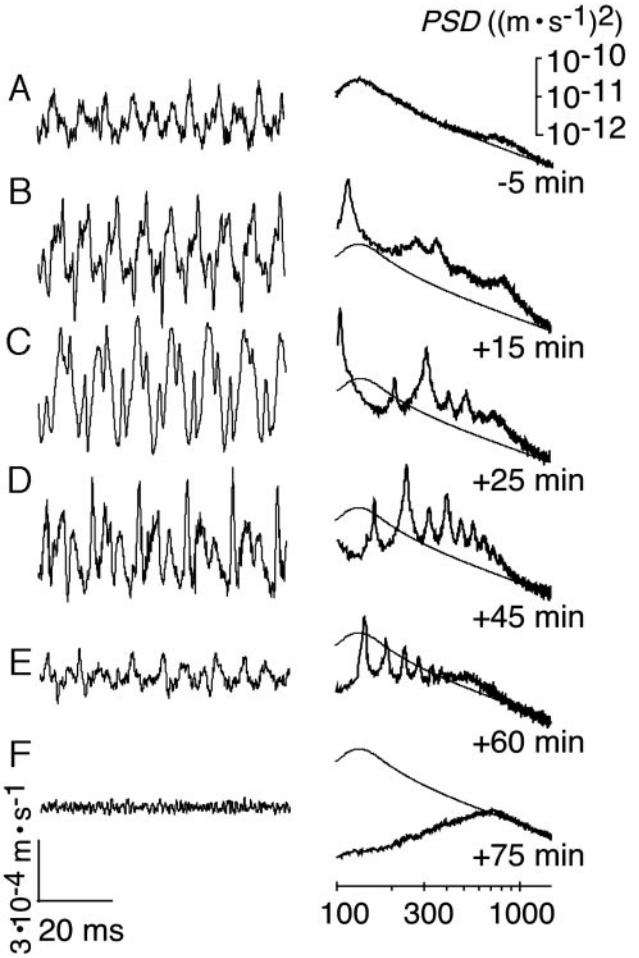

Fig. 3. Spontaneous oscillations in WT flies and facilitation by DMSO. Time traces (*Left*) and power spectra (*Right*) of the vibration velocity of an individual receiver measured 5 min before injection of DMSO (*A*) and afterward (*B–F*). PSD, power spectral density. Thin line (repeated in each image), function of a simple harmonic oscillator fitted to the spectrum in *A*. Change in power relative to *A*: 996% (*B*), 1,767% (*C*), 759% (*D*), 70% (*E*), and 11% (*F*).

ible. After CO_2 exposure, responses to faint sounds reverted back to lower frequencies, restoring the initial nonlinearity within ≈80 s (Fig. 2). These results demonstrate the presence of a physiologically vulnerable mechanism in the *Drosophila* auditory system that modulates the mechanical response of the receiver to sound. Reducing stiffness as intensity declines, this mechanism shifts down the resonance of the receiver toward the frequencies that dominate the song of the fly [160–210 Hz (16, 19)].

Spontaneous Oscillations. To assess whether the nonlinearity of the receiver associates with oscillation activity, we measured the fluctuations of the receiver in the absence of sound. Under these conditions, the receivers of WT flies twitched spontaneously. The waveform of these twitching oscillations was nonsinusoidal, displaying limit cycles that consisted of alternating rapid strokes and slower components (Fig. 3*A*). With f_Rs = 207 ± 49 Hz (n = 7), these twitching oscillations were resonantly tuned to fly songs. The spontaneous twitches suggest that the receiver is driven by an active push–pull mechanism rather than solely exhibiting thermal fluctuations. Facilitation of the twitches by DMSO supports this notion. DMSO, a local analgesic (26), reportedly affects mechanosensory transduction and spike generation in insect mechanosensory neurons (27) and induces feedback oscillations in the mosquito auditory system (11). After thoracic microinjection of DMSO [30%, dissolved in saline (11)], the twitching oscillations of the antennal receiver of the fly gained in regularity and large amplitude limit cycles emerged (Fig. 3 *B* and *C*). Simultaneously, the resonance peak observed in frequency spectra increased in height, and the oscillation power, calculated as the total power spectral density at frequencies between 100 and 1,500 Hz, increased up to 18-fold (animal in Fig. 3*C*). The limit cycles typically persisted for 1 h (Fig. 3 *B–F*). During this time, their waveform gradually distorted and the power continuously dropped, falling below its initial value (Fig. 3*E*). Finally, the limit cycles disappeared with the death of the animal, revealing the postmortem fluctuations of the receiver (Fig. 3*F*). These fluctuations exhibited the expected resonant tuning with f_R = 792 ± 36 Hz (n = 7), and their power was 9 times less than before treatment (Fig. 3 *A* and *F*). Collectively, such mechanical effects cannot be observed in a passive system. The waveform of the spontaneous oscillations, their facilitation, the resulting power gain, and the pronounced postmortem drop in oscillation power show that *Drosophila* actively shakes its antennal receiver.

Origin of Nonlinearity and Spontaneous Oscillations. The source of auditory motion generation was traced by analyzing the mechanics of the receiver in *nompA*^{2} mutants (24, 28). *nompA* encodes an extracellular linker protein located in the extracellular caps (Fig. 4*A*) that connect the ciliated dendrites of the auditory mechanosensory neurons to the antennal receiver (28). Disconnecting the neurons from the receiver, mutations in *nompA* result in conductive hearing loss (15, 28). Our analysis revealed that the receiver of *nompA*^{2} mutants exhibits a linear response and fails to twitch spontaneously. Although controls displayed nonlinear WT responses, responses to different stimulus intensities superimposed in the mutants (Fig. 4*A*). In *nompA*^{2} flies, linearization took place at f_Rs = 430 ± 27 Hz (Fig. 4*B*), with the low frequency probably reflecting the drop in the stiffness of the receiver caused by the disconnection of neurons. A resonance at corresponding frequencies was detected when the fluctuations of the receiver were measured in the absence of sound (Fig. 5). Notably, despite the low f_R, the oscillation power was considerably lower than in controls, closely resembling that of dead WT flies (Fig. 6). Moreover, in *nompA*^{2} mutants, the resonant fluctuations of the receiver were not accompanied by limit cycles, neither were they affected by DMSO (Fig. 5). Hence, when disconnected from the neurons, the mechanics of the antennal receiver is linear and passive. Nonlinearity and oscillation activity are introduced by neurons.

The neural basis of auditory motion generation is supported by the mechanics of the receiver in *nompC*^{2} mutants (24, 29). *nompC* encodes a mechanosensory transduction channel (29) that accounts for about half the compound electrical response of the mechanosensory neurons in the auditory system of the fly (15). In *nompC*^{2} mutants, the nonlinearity of the receiver was markedly reduced (Fig. 4*A*). When the stimulus particle velocity was decreased from 10^{-3} to 10^{-5} m/s, f_R shifted down from 634 ± 30 Hz to 579 ± 20 Hz (Δ = 55 Hz) in the mutants and from 791 ± 26 Hz to 402 ± 11 Hz (Δ = 389 Hz) in controls (Fig. 4*B*). The slopes of the shift were 1.4 and 9.7 Hz/dB for mutants and controls, respectively (Fig. 4*B*). This partial linearization coincided with a reduced oscillation activity. In *nompC*^{2} mutants, the power of the spontaneous oscillations of the receiver was nearly 4 times less than in controls (Figs. 5 and 6). Instead of the single resonance observed in responses to sound, the spontaneous oscillations displayed several broad peaks (Fig. 5). After DMSO administration, these peaks moved in frequency and gradually disappeared. Postmortem, a single resonance at f_R = 740 ± 38 Hz (n = 7) remained, and the oscillation power was about half that before treatment, resembling that observed in dead WT

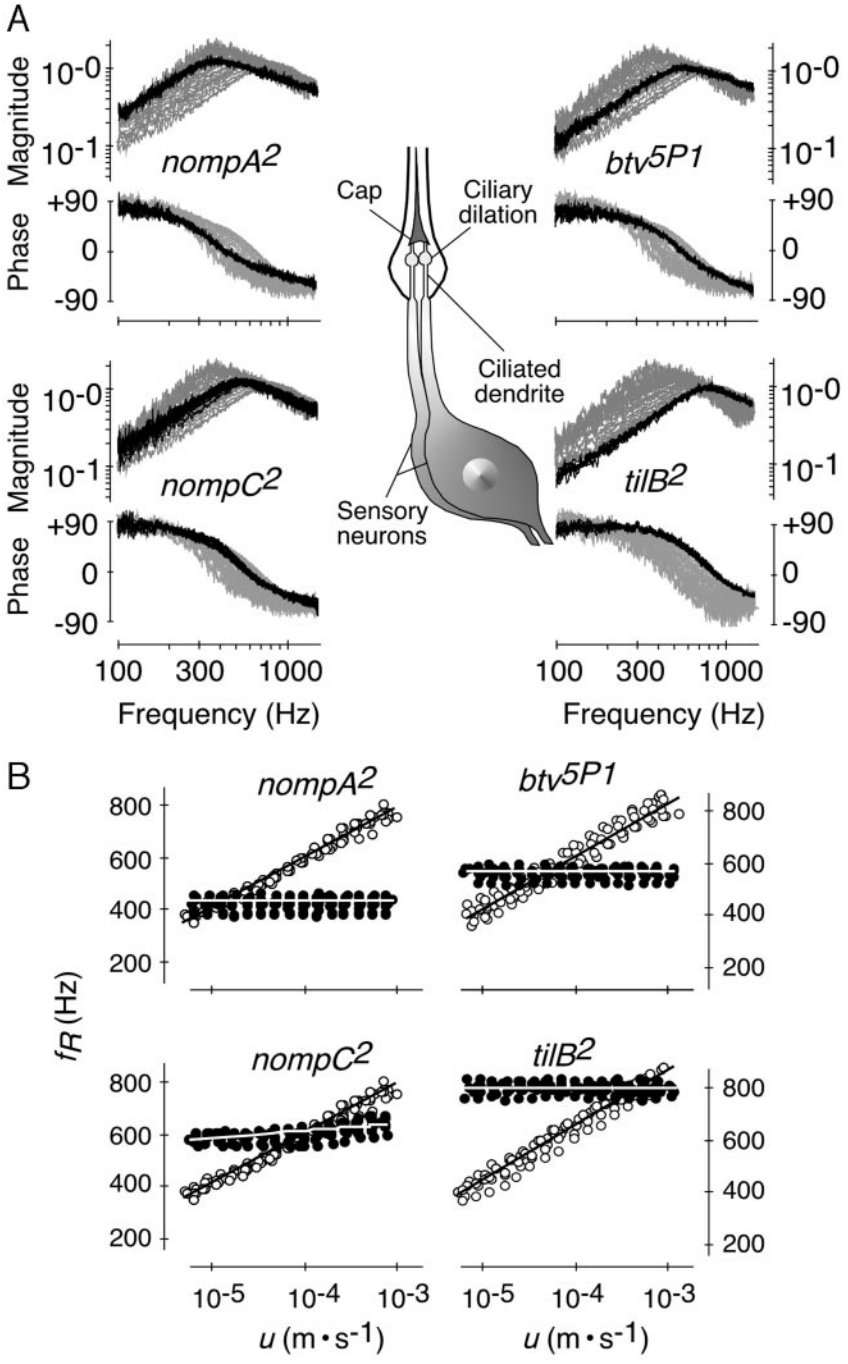

Fig. 4. Linearization of the mechanical response of the receiver in mechanosensory mutants. (*A*) Sketch of an auditory sensillum (*Center*) and images depicting superimposed responses to different stimulus particle velocities *u* for mutants (black traces) and respective controls (ghost traces) (stimuli and axis labeling as in Fig. 1*B*). The auditory sensilla of the fly each comprise two to three neurons, the ciliated of which are dilated distally and connect to the antennal receiver via an extracellular cap. (*B*) f_R as a function of *u* for mutants (●) and respective controls (○) ($n = 7$ per strain). Lines, average logarithmic curve fits; slopes, $nompA^2 = 0.0 \pm 0.1$ Hz/dB ($r^2 = 0.05 \pm 0.08$, $P > 0.05$) and control $= 9.7 \pm 0.8$ Hz/dB ($r^2 = 0.99 \pm 0.00$, $P < 0.001$); $nompC^2 = 1.4 \pm 0.3$ Hz/dB ($r^2 = 0.78 \pm 0.10$, $P < 0.001$) and control as for $nompA^2$; $btv^{5P1} = 0.1 \pm 0.1$ Hz/dB ($r^2 = 0.11 \pm 0.14$, $P > 0.05$) and control $= 10.0 \pm 0.7$ Hz/dB ($r^2 = 0.99 \pm 0.00$, $P < 0.001$); and $tilB^2 = 0.0 \pm 0.2$ Hz/dB ($r^2 = 0.16 \pm 0.12$, $P > 0.05$) and control $= 10.5 \pm 0.7$ Hz/dB ($r^2 = 0.99 \pm 0.00$, $P < 0.001$).

flies (Fig. 5). The reduced nonlinearity and oscillation activity in $nompC^2$ mutants mean that motion generation by *Drosophila* mechanosensory neurons depends on the functionality of mechanosensory transduction channels.

Complete loss of auditory motion generation, as found in $nompA^2$ flies, results from mutations in two further genes, *btv* and *tilB*. In btv^{5P1} and $tilB^2$ mutants (24, 25), the response was linear, whereas controls showed nonlinear WT responses (Fig. 4*A*). f_Rs were 539 ± 22 Hz for btv^{5P1} and 770 ± 22 Hz for $tilB^2$ (Fig. 4*B*), the latter figure closely matching the f_R of dead WT flies. Resonant fluctuations at corresponding frequencies occurred in the absence of acoustic stimuli (Fig. 5). Yet, fluctuation power was low (Figs. 5 and 6), and the fluctuations were neither accompanied by limit cycles nor affected by DMSO (Fig. 5). Deafness in btv^{5P1} and $tilB^2$ mutants associates with ciliary defects (15, 20). In btv^{5P1} mutants, the dendritic cilia of auditory

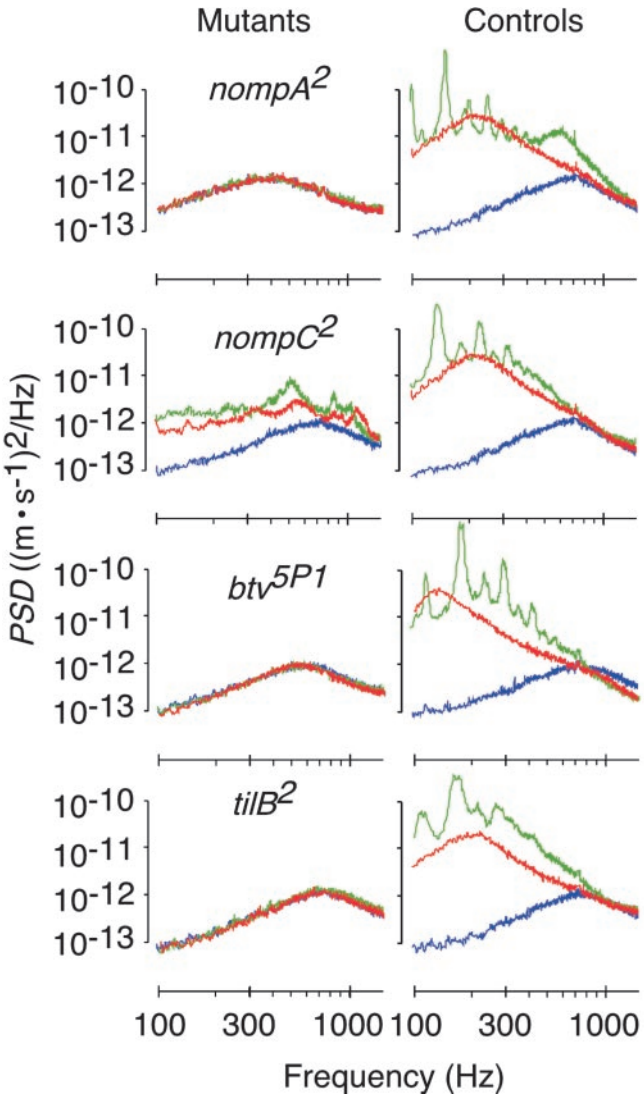

Fig. 5. Deprivation of spontaneous oscillations in mechanosensory mutants. Power spectra of the spontaneous fluctuations of the receiver in mutants (*Left*) and controls (*Right*) subsequently measured 5 min before injection of DMSO (red) as well as 40 (green) and 90 (blue) min afterward. Representative measurements from individuals chosen from $n = 7$ per strain. Change in power relative to the initial (red) fluctuations: *nompA*^{2} 98% (green) and 103% (blue), control 724% and 18%; *nompC*^{2} 152% and 54%, control 496% and 15%; *btv*^{5P1} 97% and 98%, control 1,561% and 17%; and *tilB*^{2} 96% and 101%, control 907% and 22%.

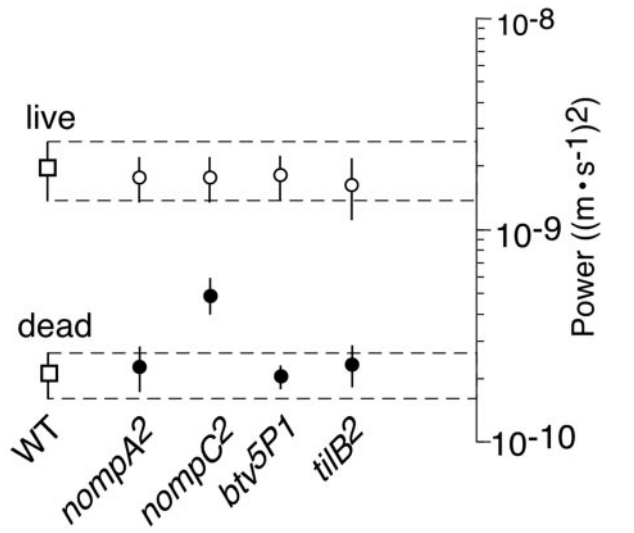

Fig. 6. Reduction of the oscillation power of the receiver in mechanosensory mutants. The oscillation power for live mutants (●) and respective controls (○) is compared with that of live and dead WT flies (□) (mean ± SD; seven flies per strain). Power is given as the total power spectral density in the frequency interval between 100 and 1,500 Hz. Hatched lines (±SD for WT flies) provide fiducials against which to judge differences in oscillation power.

mechanosensory neurons display an anatomically aberrant ciliary dilation (ref. 15; Fig. 4*A*), the contact zone between ciliary axoneme and membrane, and, possibly, the site of mechanosensory transduction (30). Mutations in *tilB* are deemed to affect dendritic cilia because of their effects on sperm (15, 20). *tilB*^{2} mutants, in addition to being deaf, fail to produce motile sperm. Their spermatid axonemes lack dynein arms (15), the very microtubule-dependent motors that account for ciliary motility. The loss of the nonlinearity and oscillation activity of the receiver and the resulting dead WT-like auditory mechanics in *tilB*^{2} mutants thus suggest that motion generation by the mechanosensory neurons of the fly involves mechanical activity of ciliated dendrites and ciliary motors, unveiling an uncanny resemblance between neurons and sperm.

Discussion

This study documents motion generation by mechanosensory neurons in the auditory system of *D. melanogaster*. The mechanical signatures of this motion generation point to parallels with the hair bundle motility known from lower tetrapod hair cells. First, like the mechanosensory neurons of the fly, hair bundles nonlinearly alter their stiffness with the stimulus intensity. The bundles become more compliant as intensity declines (31). Second, hair bundles twitch spontaneously (32). The waveform of these active motions closely resembles the limit cycles measured on the antennal receiver of the fly (Fig. 3*B*). Third, hair bundle motility is linked to mechanosensory transduction and can be explained by the interplay between stiffness instabilities and an adaptation motor (31). Tightly linked motion generation and transduction also characterize the auditory neurons of the fly. According to a recently proposed model (22), the transduction machinery of ciliated insect mechanoreceptors involves adapting and nonadapting transduction channels that are flexibly suspended between an extracellular anchor and the cilium. NompC is an adapting mechanosensory transduction channel (29). NompA may serve as the extracellular anchor (22, 28). Btv and TilB, in turn, are required for the functionality of dendritic cilia and ciliary motility (15). Hence, in *Drosophila*, motion generation by mechanosensory neurons relies on prominent molecular components of the mechanosensory transduction machinery.

Two candidate motors that may bring about hair bundle motility have been proposed: a myosin-based motor and a channel-based motor, the latter involving Ca^{2+}-dependent reclosure motions of mechanosensory transduction channels (3, 7). In *Drosophila*, the present evidence points to yet another, ciliary motor. Such a possibility, which conforms to indications that the cilia of insect mechanosensory neurons bend during transduction (33), is interesting. The ciliary axoneme of these neurons displays the "9 + 0" microtubule arrangement characteristic of primary cilia (30). Lacking central axonemal microtubules, these cilia are generally assumed to be immotile, with rare exceptions such as the solitary cilia in the immature rabbit oviductal epithelium (34) and nodal cilia in the mouse (35). Apart from promising insights into this unconventional form of ciliary motion generation, the combined genetic and biomechanical dissection of *Drosophila* audition will be useful twice: by providing the means for understanding the intricate molecular mechanisms neurons em-

ploy to detect motions and, complementarily, how detection is improved by the motility of neurons.

We thank Dr. M. J. Kernan (State University of New York, Stony Brook) for *nompA*[2] and *nompC*[2] mutants and background; Dr. D. F. Eberl (University of Iowa, Iowa City) for *btv*[5P1] and *tilB*[2] mutants and backgrounds; D. Eberl, E. Hafen, and H. Stocker for valuable discussions; B. Porter for technical assistance; and Drs. M. C. Holley, A. D. L. Humphris, G. A. Manley, R. N. Miles, and J. Ogden for comments on the manuscript. This work was supported by research fellowships from the Royal Society London and the Deutsche Akademie der Naturforscher Leopoldina (to M.C.G.) and by grants from the Swiss National Science Foundation and the University of Bristol (to D.R.).

1. Hudspeth, A. J. (1989) *Nature* **341,** 397–404.
2. Dallos, P. (1992) *J. Neurosci.* **12,** 4575–4585.
3. Hudspeth, A. J. (1997) *Curr. Opin. Neurobiol.* **7,** 480–486.
4. Nobili, R., Mammano, F. & Ashmore, J. (1998) *Trends Neurosci.* **21,** 159–167.
5. Holley, M. C. (1996) in *The Cochlea*, ed. Dallos, P. (Springer, New York), pp. 387–434.
6. Robles, L. & Ruggero, M. A. (2001) *Phys. Rev.* **81,** 1305–1352.
7. Hudspeth, A. J., Choe, Y., Metha, A. D. & Martin, P. (2000) *Proc. Natl. Acad. Sci. USA* **97,** 11765–11772.
8. Manley, G. A. (2001) *J. Neurophysiol.* **86,** 541–549.
9. Probst, R. (1990) in *New Aspects of Cochlear Mechanics and Inner Ear Pathophysiology*, ed. Pfaltz, C. R. (Karger, Basel), pp. 1–91.
10. Köppl, C. (1995) in *Advances in Hearing Research*, eds. Manley, G. A., Klump, G. M., Köppl, C., Fastl, H. & Oeckinghaus, H. (World Scientific, Singapore), pp. 201–216.
11. Göpfert, M. C. & Robert, D. (2001) *Proc. R. Soc. London Ser. B* **268,** 333–339.
12. Kernan, M. & Zuker, C. (1995) *Curr. Opin. Neurobiol.* **5,** 443–448.
13. Kössl, M. & Boyan, G. S. (1998) *Naturwissenschaften* **85,** 124–126.
14. Eberl, D. F. (1999) *Curr. Opin. Neurobiol.* **9,** 389–393.
15. Eberl, D. F., Hardy, R. W. & Kernan, M. J. (2000) *J. Neurosci.* **20,** 5981–5988.
16. Bennet-Clark, H. C. (1971) *Nature* **234,** 255–259.
17. Hall, J. C. (1994) *Science* **264,** 1702–1714.
18. Greenspan, R. J. & Ferveur, J. F. (2000) *Annu. Rev. Genet.* **34,** 205–232.
19. Göpfert, M. C. & Robert, D. (2002) *J. Exp. Biol.* **205,** 1199–1208.
20. Caldwell, J. C. & Eberl, D. F. (2002) *J. Neurobiol.* **53,** 172–189.
21. Göpfert, M. C. & Robert, D. (2001) *Nature* **411,** 908.
22. Gillespie, P. G. & Walker, R. G. (2001) *Nature* **413,** 194–202.
23. Jarman, A. P. (2002) *Hum. Mol. Genet.* **11,** 1215–1218.
24. Kernan, M., Cowan, D. & Zuker, C. (1994) *Neuron* **12,** 1195–1206.
25. Eberl, D. F., Duyk, G. M. & Perrimon, N. (1997) *Proc. Natl. Acad. Sci. USA* **94,** 14837–14842.
26. Sawada, M. & Sato, M. (1975) *Ann. N.Y. Acad. Sci.* **243,** 337–357.
27. Theophilidis, G. & Kravari, K. (1994) *Neurosci. Lett.* **181,** 91–94.
28. Chung, Y. D., Zhu, J., Han, Y.-G. & Kernan, M. (2001) *Neuron* **29,** 415–428.
29. Walker, R. G., Willingham, A. T. & Zuker, C. S. (2000) *Science* **287,** 2229–2234.
30. Field, L. H. & Matheson, T. (1989) *Adv. Insect Physiol.* **27,** 1–228.
31. Martin, P., Mehta, A. D. & Hudspeth, A. J. (2000) *Proc. Natl. Acad. Sci. USA* **97,** 12026–12031.
32. Martin, P. & Hudspeth, A. J. (1999) *Proc. Natl. Acad. Sci. USA* **96,** 14306–14311.
33. Moran, D. T., Varela, F. J. & Rowley, J. C., III (1977) *Proc. Natl. Acad. Sci. USA* **74,** 793–797.
34. Odor, D. L. & Blandau, R. J. (1985) *Am. J. Anat.* **174,** 437–453.
35. Nonaka, S., Tanaka, Y., Okada, Y., Takeda, S., Harada, A., Yoshimitsu, K., Kido, M. & Hirokawada, N. (1998) *Cell* **95,** 829–837.